Frequency-Based Load Control in Power Systems

Changhong Zhao*, Ufuk Topcu* and Steven H. Low*
*Division of Engineering and Applied Science
California Institute of Technology, Pasadena, California 91125

Abstract—**Maintaining demand-supply balance and regulating frequency are key issues in power system control. Conventional approaches focus on adjusting the generation so that it follows the load. However, relying on solely regulating generation is inefficient, especially for power systems where contingencies like sudden loss in generation or sudden change in load frequently occur and the proportion of intermittent renewable power is increasing. We present a frequency-based load control scheme for demand-supply balancing and frequency regulation. We formulate a load control optimization problem which aims to balance the change in load with the change in supply while minimizing the overall end-use disutility. By studying the power system model that characterizes the frequency response to real power imbalance between demand and supply, we design decentralized synchronous and asynchronous algorithms which take advantage of local frequency measurements to solve the load control problem. Case studies show that the proposed load control scheme is capable of relatively quickly balancing the power and restoring the frequency under generation-loss like contingencies or renewable power penetration. Case studies also show that the proposed scheme still works well when users have the knowledge of a simplified system model instead of an accurate one.**

I. INTRODUCTION

In power systems, the imbalance between generation and load must get corrected within short periods, otherwise it will drive the power line frequency to deviate from the nominal value (e.g., 60 Hz). Large frequency deviation may threaten the stability and security of the power system, or even worse, cause permanent damage to the facilities [1][2]. Hence balancing generation with load and regulating frequency at the normal level has been a significant topic in power system operations.

Multiple control approaches have been applied to serve these goals. Conventional control efforts focus on the generation side. For example, the automated generation control (AGC) issues signals to control the reserved generation capacity and minimize the area control error (ACE), which includes both frequency deviation and unscheduled tie-line power flows [3][4]. The spinning reserve is a set of frequency responsive generators that automatically increase their output when a sudden loss of supply occurs [3]. In addition, many generators are equipped with speed governors which adjust the mechanical power proportionally to the frequency deviation [5][7]. Other control components include the exciter and the power system stabilizer (PSS) [8][9].

Generation side control, though widely used, has many inadeqancies. For example, the AGC takes as long as 5-15 minutes to drive the ACE to its setpoint [4]. The spinning reserve generators cannot immediately respond to a contigency, and they must be grid connected and operating in a part-loaded state, thus increasing the cost and emissions [3]. The speed governor typically has a droop characteristic so that it cannot eliminate the steady state frequency deviation [8]. Today, purely relying on the generation control is not only prohibitively expensive but also technically difficult [10]. As a complementary, a lot of works have investigated the potential of load participation in power system control, among which the load control based on local frequency measurement has been highlighted.

Loads are typically controlled via load-shedding, where a whole region of loads are disconnected from the grid by a underfrequency load-shedding (UFLS) relay as a last resort to avoid system failure [2][12]. However, additional granularity can be achieved by individual loads to be controlled. Loads with energy storage, such as heaters, air conditioners, refrigerators and PEVs, can be modulated with reasonable disturbance to customer comforts [11], so they are good candidates for load control. Equipped with frequency sensors, they can sense the frequency as a measure of supply-demand imbalance, and respond in less than 1 second [13].

Schweppe *et al.* presented the idea of individual load control through responding to frequency as early as 1979 [14][15]. Taylor *et al.* developed a distributed fuzzy load controller for renewable energy systems, which uses both the frequency and the rate of change of frequency to minimize the frequency deviations [16][17]. Trudnowski *et al.* assumed the loads can be adjusted proportionally to frequency deviations, and investigated multiple issues such as the distribution of loads, time delay and discretized load action [5][6]. Molina-Garcia *et al.* studied the aggregated load response characteristics when each load is turned on and off as the frequency goes across some thresholds [2]. The Grid Friendly Appliance controller [18] developed by the Pacific Northwest National Laboratory suggests that individual appliances can provide fast reserve within seconds by responding to certain trends in the frequency.

All the works above show the advantage of frequency-based load control that communication between loads and a central controller is no longer essential and the control is decentralized, since each load can measure the frequency signal locally. However, these works are mostly based on experiments, and do not prove convergence of their decentralized schemes. Moreover, they do not consider the user acceptance as a system-level requirement. An acceptable control strategy should affect end-use functions as little as possible, otherwise users may withdraw from the control program and the reserve capacity may decrease [3].

In this paper, we maintain the advantage that local frequency measurements decentralize the load control. In addition, we address the user acceptance issue by formulating an load control optimization problem whose objective is to minimize the overall end-use disutility and whose constraint is the demand-supply power balance. To solve the problem, we develop a synchronous algorithm which assumes all loads sense the frequency without measurement delays and make decisions synchronously, and then consider a more practical asynchronous algorithm which incorporates frequency measurement delay and asynchronous decision making. We prove the convergence of the proposed algorithms, with which the load control problem can be solved in a decentralized way. Besides, we discuss the effect of using a simplified system model instead of an accurate one, since in practice users may not get the exact knowledge of the system model and a simplified model can make modeling and computation easier. Numerical experiments show that the proposed load control scheme is able to drive demand-supply imbalance and frequency deviation to zero within 10 to 20 seconds after a sudden generation loss, and is relatively effective in regulating frequency and maintaining demand-supply balance under fluctuating wind generation. Moreover, the proposed scheme works well when a simplified system model, instead of an accurate one, is used.

This paper is organized as follows. Section II describes the system model and sets up the load control optimization problem. Section III presents the load control algorithms and proves their convergence. Section IV shows the case studies, including system settings and the results of numerical experiments. Section V discusses the limitations in the proposed scheme, and suggests several possible directions for future work. Finally, Section VI concludes the paper.

II. MODEL AND PROBLEM SETUP

In this section we introduce the power system model upon which the frequency-based load control scheme is built. Then we formulate an optimization problem that describes two goals of load control: minimizing the overall end-use disutility caused by change in load, and balancing demand with supply.

A. System model

Figure 1 shows the schematic diagram of the power system under consideration. On the generator side, multiple control approaches regulate the magnitude of stator voltage $|E_a'|$, the rotor angle δ, the frequency $\omega = d\delta/dt$ and the terminal voltage V_a. For example, the exciter adjusts the field-winding voltage E_{fd} based on the measurement of V_a; the speed governor adjusts the mechanical power P_m based on the measurement of ω. Electrical power P_e is supplied to the load bus via the transmission line. Let $I = \{1, 2, ...N\}$ denote the set of loads or users (we use these two terms interchangeably). Each load $i \in I$ consumes real power d_i which is regulated by a controller LC_i. Δg denotes a real power disturbance which causes demand-supply imbalance and frequency deviation. For example, Δg may be unscheduled power flow from another
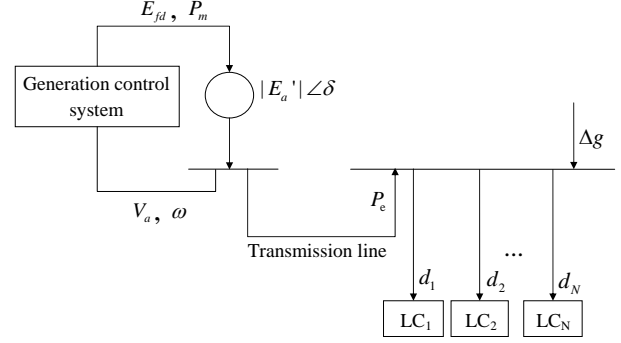

Fig. 1. Schematic diagram of the system under consideration. $|E_a'|$ is the magnitude of generator stator voltage, δ is the rotor angle. The generation control system measures the terminal voltage V_a and frequency ω, and adjusts the field-winding voltage E_{fd} and the turbine mechanical power P_m. P_e is the power supplied to the loads. Each load $i \in \{1, ..., N\}$ is equipped with a load controller LC_i that modulates load power d_i when a power disturbance Δg occurs.

bus, power supplied by a renewable generation source, a sudden load change, or a sudden generation loss. The case $\Delta g > 0$ may stand for the increase of supply or the decrease of load.

For each $i \in I$, LC_i measures the frequency deviation from the nominal value (e.g., 60 Hz), $\Delta\omega$, and calculates the change in load Δd_i. Let $\Delta d_i > 0$ stand for decreasing the load power, then the total load change is $\Delta d = -\sum_{i \in I} \Delta d_i$. Define $u := \Delta d - \Delta g$, which is actually the demand-supply power imbalance. Then we have a system process that characterizes the relation between frequency deviation $\Delta\omega$ and power imbalance u. We linearize the process around some operating point, get a linear model M and describe M by a transfer function $G(s)$ such that $\Delta\omega(s) = G(s)u(s)$, as is a usual approach to simplify the power system analysis [22][23]. Note that M is continuous-time, while the load control system is a sampling control system, i.e., users sample $\Delta\omega$ and make decisions once every Δt time, and hold their decisions within the sampling interval. We use $t \in T = \{1, 2, ...\}$ instead of $t = \Delta t, 2\Delta t, ...$ to denote the time. Including the samplers and holders in M, we have a discrete-time realization, denoted by $\{A, B, C\}$, such that

$$\begin{aligned} x_{t+1} &= Ax_t + Bu_t \\ \Delta\omega_t &= Cx_t, \end{aligned} \tag{1}$$

where $x \in \mathbb{R}^n$ is the state vector, $A \in \mathbb{R}^{n \times n}$, $B \in \mathbb{R}^{n \times 1}$, and $C \in \mathbb{R}^{1 \times n}$.

Note that $\{A, B, C\}$ exists if the transfer function $G(s)$ has a continuous-time realization (at least one exists, e.g. in the canonical form [28]), denoted by $\{A_c, B_c, C_c\}$, such that

$$\begin{aligned} \dot{x}(t) &= A_c x(t) + B_c u(t) \\ \Delta\omega(t) &= C_c x(t), \end{aligned} \tag{2}$$

and A_c is non-singular with all the eigenvalues having negative real parts. To see this, note that u is held constant within the

sampling interval, so

$$A = e^{A_c \Delta t},$$
$$B = A_c^{-1}(A - I_n)B_c,$$
$$C = C_c.$$

Moreover, in the load control scheme proposed later, we require the condition $CB \neq 0$ (see (10)), which holds for the models we use as a partial justification. Hence we make the following assumption.

Assumption 1. There exists a realization $\{A, B, C\}$ of the system process model M such that $CB \neq 0$.

With the model introduced above, we now formulate an optimization problem that captures the goals of our load control scheme.

B. Load control optimization problem

The goal of the load control scheme proposed here is to balance power demand and supply, i.e., to drive u to zero. By $\Delta\omega(s) = G(s)u(s)$, the frequency deviation will be driven to zero if u is zero. The proposed control scheme simultaneously takes end-use functions as a system-level consideration, by minimizing the overall disutility caused by changing the loads.

We consider a constant Δg, and without loss of generality, assume $\Delta g < 0$. Each user $i \in I$ has a disutility value $D_i(\Delta d_i)$ which is a function of $\Delta d_i \in [0, \bar{d}_i]$, where $\bar{d}_i$ is the maximum change in load i allowed by appliance design or user permission. Considering the goal of minimizing overall disutility and making $u = 0$, given the disturbance Δg and the set of users I, we formulate the following load control problem, denoted by **PP**.

$$\mathbf{PP} \begin{cases} \min\limits_{\Delta d_i \in [0, \bar{d}_i]} & \sum\limits_{i=1}^{N} D_i(\Delta d_i) \\ \text{subject to} & -\sum\limits_{i=1}^{N} \Delta d_i - \Delta g = 0. \end{cases}$$

For feasibility of **PP**, we need $-\sum_{i \in I} \bar{d}_i < \Delta g$, i.e., the magnitude of disturbance does not exceed the capability of changing the loads, which is true if enough loads participate in the load control scheme. We make the following two assumptions on the disutility functions D_i.

Assumption 2. For $i \in I$, D_i is increasing, strictly convex and twice continuously differentiable over $[0, \bar{d}_i]$.

Assumption 3. For $i \in I$, there exists $\bar{\alpha}_i > 0$ so that $D_i''(\Delta d_i) \geq 1/\bar{\alpha}_i$ for $\Delta d_i \in [0, \bar{d}_i]$.

With Assumptions 2-3, **PP** becomes a convex problem which can be solved using the decentralized approach proposed later. Moreover, the reasonability of Assumptions 2-3 can be implied from previous works on demand response, where the utility functions are non-decreasing and concave, which means users are interested to consume more power if possible, and the level of satisfaction for users can gradually get saturated. For example, the utility functions often take the quadratic form and have linear marginal benefits [30][31].

Solving **PP** by a central controller requires the knowledge of D_i for all $i \in I$. However, for privacy considerations, users may not prefer to reveal their disutility functions to the utility company or any other organization that controls the system. Moreover, the disutility functions may take a complex form and change with time, so it would cost much to communicate the disutility fucntions to a central controller. Therefore, we propose a decentralized approach to solve **PP**. In order to derive this decentralized procedure, we consider the dual problem of **PP**. Define the Lagrangian of **PP**

$$L(\Delta d_i, p) := \sum_{i=1}^{N} D_i(\Delta d_i) + p\left(-\sum_{i=1}^{N} \Delta d_i - \Delta g\right).$$

Then, the dual objective function is

$$\begin{aligned} U(p) &= \inf_{\Delta d_i \in [0, \bar{d}_i]} L(\Delta d_i, p) \\ &= \sum_{i=1}^{N} \min_{\Delta d_i \in [0, \bar{d}_i]} (D_i(\Delta d_i) - p\Delta d_i) - p\Delta g. \end{aligned} \quad (3)$$

Hence, we have the dual problem, denoted by **DP**.

$$\mathbf{DP} \left\{ \quad \max_p \ U(p). \right.$$

The solution to **PP** can be constructed in a decentralized way, from **DP**. To see this, note that given $p \in \mathbb{R}$, the problem

$$\min_{\Delta d_i \in [0, \bar{d}_i]} D_i(\Delta d_i) - p\Delta d_i \quad (4)$$

has a unique minimizer denoted by

$$\Delta d_i(p) = \min\{\max\{(D_i')^{-1}(p), 0\}, \bar{d}_i\}, \quad (5)$$

since D_i is strictly convex. Note that the inverse of D_i' exists over $[D_i'(0), D_i'(\bar{d}_i)]$ since D_i' is continuous and strictly increasing by Assumption 2. Since D_i is convex for $i \in I$ and **PP** has affine constraints, Slater's condition implies that there is zero duality gap between **PP** and **DP**, and the dual optimal solution, denoted by p^*, is attained [26, Sec. 5.5.3]. It follows that $d(p^*) := [d_1(p^*), ..., d_N(p^*)]^T$ is primal feasible and optimal [26, Sec. 5.5.2]. Therefore, we can focus on solving the dual problem **DP** to solve **PP**, instead of solving **PP** directly.

III. FREQUENCY-BASED LOAD CONTROL ALGORITHMS

In this section, we first introduce an input reconstructor which forms the basis of the frequency-based load control algorithms by reconstructing the input u to the system (which is actually the gradient value of the dual objective function) locally at each load and enabling solving **DP** with a decentralized gradient method. Then we introduce the algorithms, including a synchronous version and an asynchronous version. In the algorithms, each user solves its local problem, so that the changes in the loads converge to the solution of the load control problem **PP**.

A. Input reconstructor

As introduced in Section II-B, given the maximizer of **DP**, denoted by p^*, the optimal change in load i is $\Delta d_i(p^*)$. On the other hand, we can get p^* using the gradient algorithm [20, Sec. 3.2.1], where at each time t the value of p is adjusted in the direction of the gradient $U'(p)$ as

$$p(t+1) = p(t) + \gamma U'(p(t)), \tag{6}$$

where $\gamma > 0$ is a stepsize. Recall that $\Delta d_i(p)$ denotes the unique minimizer of (4) for given p. By (3), if the change in load i at time t is $\Delta d_i(t) = \Delta d_i(p(t))$,[1] we have

$$U'(p(t)) = -\sum_{i=1}^{N} \Delta d_i(t) - \Delta g = u_t, \tag{7}$$

where u_t denotes the value of demand-supply imbalance u at time t. Substituting (7) into (6) we have

$$p(t+1) = p(t) + \gamma u_t. \tag{8}$$

Therefore, the key to decentralizing the load control is to reconstruct the value of u locally at each load. Since u is the input to the power system modeled by M (see Section II-A), we call the mechanism of reconstructing u as the input reconstructor. In the frequency-based load control scheme, the input reconstructor takes advantage of local frequency measurement, $\Delta\omega$, to reconstruct u. For load $i \in I$, the estimate of the state vector x_t using frequency measurements up to time $(t-1)$ is denoted by $\hat{x}_{t|t-1}^i$, the estimate of x_t using frequency measurements up to time t is denoted by $\hat{x}_{t|t}^i$, and the estimate of u_{t-1} is denoted by $\hat{u}_{t-1}^i$. In the input reconstructor, $\hat{x}_{t|t-1}^i$, $\hat{x}_{t|t}^i$ and $\hat{u}_{t-1}^i$ are recursively given by

$$\hat{x}_{t|t-1}^i = A\hat{x}_{t-1|t-1}^i, \tag{9}$$

$$\hat{u}_{t-1}^i = (CB)^{-1}(\Delta\omega_t - C\hat{x}_{t|t-1}^i), \tag{10}$$

$$\hat{x}_{t|t}^i = \hat{x}_{t|t-1}^i + B\hat{u}_{t-1}^i. \tag{11}$$

The input reconstructor presented by (9)-(11) is a special case of the unbiased minimum-variance input estimator in [24] when process noise and measurement noise are zero. The following proposition states that the input reconstructor is able to reconstruct the value of u locally at each load.

Proposition 1. Suppose Assumption 1 holds, $\hat{x}_{0|0}^i = x_0$. Then, the input reconstructor (9)-(11) gives $\hat{u}_{t-1}^i = u_{t-1}$ for all $i \in I$ at all times $t \in T$.

Proof: If $\hat{x}_{t-1|t-1}^i = x_{t-1}$, by (1), (9) and (10),

$$\begin{aligned}
\hat{u}_{t-1}^i &= (CB)^{-1}(\Delta\omega_t - C\hat{x}_{t|t-1}^i) \\
&= (CB)^{-1}(CAx_{t-1} + CBu_{t-1} - CA\hat{x}_{t-1|t-1}^i) \\
&= (CB)^{-1}CBu_{t-1} = u_{t-1}.
\end{aligned} \tag{12}$$

---

[1] We abuse the notation by referring to $\Delta d_i(\cdot)$ as a function of time on the left of the equation and a function of p on the right. The meaning should be clear from the context.

By (1), (9), (11) and (12), we have

$$\begin{aligned}
\hat{x}_{t|t}^i &= \hat{x}_{t|t-1}^i + B\hat{u}_{t-1}^i \\
&= A\hat{x}_{t-1|t-1}^i + Bu_{t-1} \\
&= Ax_{t-1} + Bu_{t-1} = x_t.
\end{aligned} \tag{13}$$

Starting from $\hat{x}_{0|0}^i = x_0$ and recursively using (12)-(13), we conclude the proof. ■

Based on the input reconstructor, we design decentralized load control algorithms.

B. Synchronous algorithm

In the synchronous algorithm, each user senses the power line frequency without measurement delay, and makes decisions synchronously at times $t \in T = \{1, 2, ...\}$. The synchronous algorithm forms the basis of the asynchronous algorithm, which will be proposed in Section III-C.

We present the synchronous algorithm as follows.

Algorithm 1. *Synchronous frequency-based load control algorithm*

For all loads $i \in I = \{1, 2, ...N\}$, the discrete-time realization of the system process model M, denoted by $\{A, B, C\}$, is given. Choose a stepsize $\gamma > 0$. Set the time $t = 0$, and initialize each load i with $\hat{x}_{0|0}^i = x_0$ and $p_i(0) = 0$.

At times $t = 1, 2, ...$, load i:

1) Measures the frequency deviation $\Delta\omega_t$, and calculates $\hat{u}_{t-1}^i$ using (9)-(11).
2) Updates the value of p_i as

$$p_i(t) = p_i(t-1) + \gamma\hat{u}_{t-1}^i. \tag{14}$$

3) Determines the change in its load

$$\Delta d_i(t) = \Delta d_i(p_i(t)), \tag{15}$$

   where $\Delta d_i(\cdot)$ is given by (5).

We make some remarks on the initialization and stop criteria of the algorithm. For the initialization, provided all the eigenvalues of the matrix A_c in the continuous-time system realization $\{A_c, B_c, C_c\}$ (see (2)) have negative real parts, the state vector x converges to the zero vector when power demand and supply are balanced. Therefore, we can set $t = 0$ when the system has operated with balanced demand and supply for a relatively long period, and set $\hat{x}_{0|0}^i = 0$ for all i. Numerical experiments show that the algorithm still converges even if $\hat{x}_{0|0}^i \neq x_0$. For the stop criteria, the algorithm can run all the time without stop until when the system model changes, or it can be stopped when $|\Delta d_i(t+1) - \Delta d_i(t)| < \epsilon$ for some $\epsilon > 0$ for all $i \in I$.

To show the convergence of Algorithm 1, we relate it to the gradient algorithm where the dual variable p is adjusted by (8). Starting with $p(0) = 0$, the gradient algorithm produces a sequence $\{p(t), t \in T\}$. Using Algorithm 1, load $i \in I$ generates a sequence $\{p_i(t), t \in T\}$. By (8), (14) and Proposition 1, $p_i(t) = p(t)$ for all $t \in T$, which implies Algorithm 1 is equivalent to the gradient algorithm if the

conditions for Proposition 1 hold. Moreover, if Assumptions 2-3 are satisfied, the dual objective function U has the properties which gurantee the convergence of the gradient algorithm. Hence Assumptions 1-3 together lead to the convergence of Algorithm 1. Define $\overline{\alpha} := \max_{i \in I} \overline{\alpha}_i$ (see $\overline{\alpha}_i$ in Assumption 3), and define $\Delta d(t) := [\Delta d_1(t), ..., \Delta d_N(t)]^T$. The following theorem states the convergence of Algorithm 1.

Theorem 1. Suppose Assumptions 1-3 hold and the stepsize γ satisfies

$$0 < \gamma < \frac{2}{\overline{\alpha} N}, \quad (16)$$

then for any $i \in I$, any limit point (at least one exists) of the sequence $\{(\Delta d(t), p_i(t)), t \in T\}$ is primal-dual optimal for problems **PP** and **DP**.

Proof: See Appendix A. ■

We now discuss the convergence rate when p^* is the unique maximizer of the dual objective function U. We omit the subscript i denoting load i since the sequence $\{p_i(t), t \in T\}$ is the same for all i. It is straightforward that

$$p(t+1) - p^* = (1 + \gamma U''(\tilde{p}(t)))(p(t) - p^*),$$

for some $\tilde{p}(t)$ between $p(t)$ and p^*. Note that $U''(\tilde{p}(t)) < 0$ since U is concave and has a unique maximizer, and $U''(\tilde{p}(t)) > -2$ by the convergence condition (16). Therefore, $|1 + \gamma U''(\tilde{p}(t))| < 1$ always holds. In addition, near p^*, the $p(t)$ converges to p^* as $t \to +\infty$ almost as fast as a geometric series with an exponent $(1 + \gamma U''(p^*))$.

Algorithm 1 assumes an ideal case that all loads sense the frequency without measurement delay and make decisions on the change in their power synchronously at every time $t \in T$. However, this may not be true in practice. Now we come to the asynchronous case, where the frequency measurement may be delayed for a random but bounded time, and not all loads make decisions simultaneously.

C. Asynchronous algorithm

In the asynchronous setting, the frequency deviation $\Delta \omega_t$ at time t is measured by load $i \in I$ at some time within the interval $[t + r(i,t) - 1, t + r(i,t))$, where $r(i,t) \in \mathbb{N}$ is a random number. In the time interval $[t - 1, t)$, load i measures a set of frequency deviation signals, denoted by $\Omega_{i,t} = \{\Delta \hat{\omega}_{i,t}^1, ..., \Delta \hat{\omega}_{i,t}^{K_{i,t}}\}$, where $K_{i,t}$ is the number of measured frequency deviation signals ($\Omega_{i,t} = \emptyset$ and $K_{i,t} = 0$ means no frequency deviation signal is measured during $[t-1, t)$). Moreover, load i is able to change its power only at a subset of the times, denoted by $T_i \subseteq T$. For the asynchronous algorithm to converge, we make the following two assumptions on $r(i,t)$ and T_i.

Assumption 4. For all $i \in I$, $t \in T$, $l \in \{1, ..., K_{i,t}\}$ and $s \in \{1, ..., t\}$, if $\Delta \hat{\omega}_{i,t}^l$ is the measurement of $\Delta \omega_s$, then $\Delta \hat{\omega}_{i,t}^{l+1}$ is the measurement of $\Delta \omega_{s+1}$. Moreover, there exists $\overline{r} \in \mathbb{N}$ such that $r(i,t) \leq \overline{r}$ for all $i \in I$ and $t \in T$.

Assumption 5. For all $i \in I$, the difference between consecutive elements of T_i is bounded.

Assumption 4 says that the delayed frequency measurements arrive by order. In other words, the frequency deviation signal that occurs first is sensed first by the load. Moreover, all frequency measurement delays are bounded by $\overline{r}$. Assumption 5 says that the time between any consecutive changes of any load is bounded.

With the setting above, we present the asynchronous load control algorithm as follows.

Algorithm 2. *Asynchronous frequency-based load control algorithm*

For all loads $i \in I = \{1, 2, ...N\}$, the discrete-time realization of the system process model M, denoted by $\{A, B, C\}$, is given. Choose a stepsize $\gamma > 0$. Set the time $t = 0$, and initialize each load i with $\hat{x}_0^i = x_0$ and $p_i(0) = 0$.

In the time interval $[t - 1, t)$ for $t = 1, 2, ...$, load i:
1) At time $(t-1)$, sets $\hat{x}_{t-1}^i(0|0) = \hat{x}_{t-1}^i$, $p_{t-1}^i(0) = p_i(t-1)$.
2) Once load i measures a new frequency deviation signal $\Delta \hat{\omega}_{i,t}^k \in \Omega_{i,t}$ for $k = 1, ..., K_{i,t}$, it calculates $\hat{u}_{t-1}^i(k)$ by

$$\hat{x}_{t-1}^i(k|k-1) = A \hat{x}_{t-1}^i(k-1|k-1)$$

$$\hat{u}_{t-1}^i(k) = (CB)^{-1}(\Delta \hat{\omega}_{i,t}^k - C \hat{x}_{t-1}^i(k|k-1))$$

$$\hat{x}_{t-1}^i(k|k) = \hat{x}_{t-1}^i(k|k-1) + B \hat{u}_{t-1}^i(k),$$

and updates the value of p by

$$p_{t-1}^i(k) = p_{t-1}^i(k-1) + \gamma \hat{u}_{t-1}^i(k). \quad (17)$$

3) At time t, sets $\hat{x}_t^i = \hat{x}_{t-1}^i(K_{i,t}|K_{i,t})$ and $p_i(t) = p_{t-1}^i(K_{i,t})$.
4) If load i is able to change its power at time t, it determines the change

$$\Delta d_i(t) = \Delta d_i(p_i(t)).$$

Otherwise, $\Delta d_i(t) = \Delta d_i(t - 1)$.

The following theorem states the convergence of Algorithm 2.

Theorem 2. Suppose Assumptions 1-5 hold and the stepsize γ satisfies

$$0 < \gamma < \frac{1}{\overline{\alpha} N/2 + 2\overline{r}},$$

then for any $i \in I$, any limit point (at least one exists) of the sequence $\{(\Delta d(t), p_i(t)), t \in T\}$ is primal-dual optimal for problems **PP** and **DP**.

Proof: See Appendix B. ■

The proposed load control algorithms are essentially the gradient algorithm, where the gradient of the dual objective function happens to be the system demand-supply imbalance u. Using the input reconstructor, the loads reconstruct the value of u purely from local frequency measurements, without any communication between the loads and a central controller.
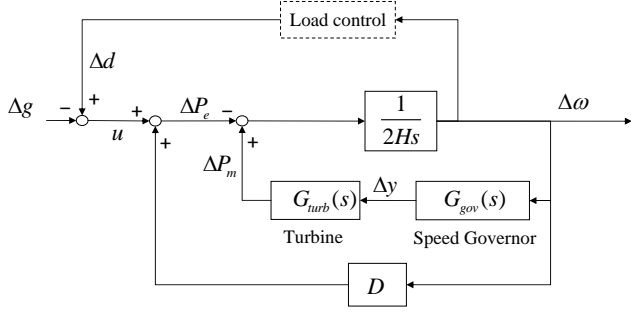
Fig. 2. Core part of the power system model, denoted by M_1. H is the generator inertia constant. D is the damping constant of motor loads. ΔP_e in the change in electrical power. The speed governor adjusts the change in turbine valve opening Δy based on the frequency deviation $\Delta\omega$, then the change in mechanical power ΔP_m is adjusted by the turbine.

Fig. 3. Complete power system model under consideration, denoted by M_2. M_2 contains M_1. Besides, the exciter adjusts the change in field-winding voltage ΔE_{fd} based on the change in terminal voltage magnitude $\Delta|V_a|$ and a signal ΔV_s from the power system stabilizer. $\Delta\delta$ is the change in rotor angle and $\Delta|E_a'|$ is the change in stator voltage magnitude.

Hence, no communication delay is involved in the proposed scheme. Moreover, the loads sense the local frequency signals with relatively small measurement delays, and respond within a short period of time. Therefore, the proposed load control scheme is able to relatively quickly balancing the demand and supply and restoring the frequency.

IV. CASE STUDIES

In this section, we use relatively detailed power system models to evaluate the performance of the proposed load control scheme. Through numerical experiments with generation-loss like contingencies, we compare between the synchronous algorithm and the asynchronous algorithm, show the impact of different numbers of loads, and discuss the effect of using a simplified system model instead of an accurate model. Since the load control under renewable generation is one of our goals to extend, we also test the proposed scheme with a fluctuating wind power generation, though no theoretical result about its performance has been proved for this case.

A. System settings

We now present the power system model under consideration. Figure 2 shows the core part of the model, denoted by M_1, which contains the swing equation, the frequency sensitivity of motor loads and the speed governor. The components in M_1 are major factors that characterize the frequency response caused by demand-supply imbalance [1][7], so we call M_1 as the core part. In M_1, the motion of generator rotor is characterized by the swing equation

$$2H\frac{d\Delta\omega}{dt} = \Delta P_m - \Delta P_e,$$

where H is the inertia constant, ΔP_m is the change in mechanical power and ΔP_e is the change in electrical power. For loads equipped with motors, the power is frequency sensitive, described by
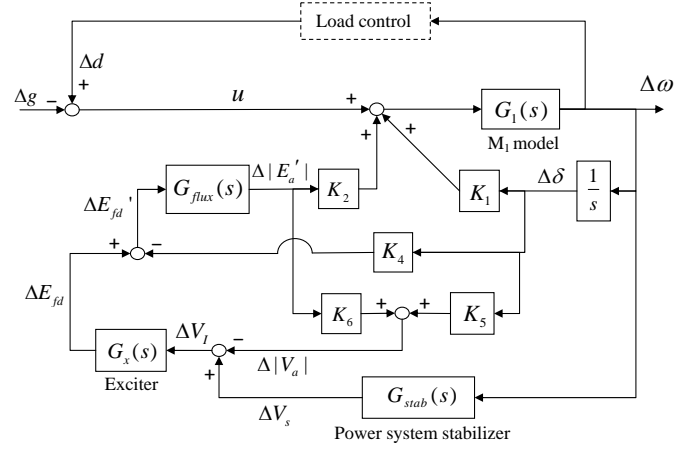
$$\Delta P_e(\Delta\omega) = D\Delta\omega,$$

where D is the damping constant. Moreover, the model contains a speed governor with the transfer function

$$G_{gov}(s) = -\frac{1}{R(1 + sT_G)}$$

such that the change in the turbine valve opening $\Delta y(s) = G_{gov}(s)\Delta\omega(s)$. The turbine has a transfer function

$$G_{turb}(s) = \frac{(1 + sF_{HP}T_{RH})}{(1 + sT_{CH})(1 + sT_{RH})}$$

such that $\Delta P_m(s) = G_{turb}(s)\Delta y(s)$. Hence, the transfer function of M_1, denoted by G_1, is

$$G_1(s) = -\frac{1/(2Hs + D)}{1 - 1/(2Hs + D)G_{turb}(s)G_{gov}(s)}. \quad (18)$$

The complete model under consideration, denoted by M_2, is shown in Figure 3. Besides the core part M_1, M_2 contains a power system stabilizer (PSS) with the transfer function

$$G_{stab}(s) = \frac{sK_w(1 + sT_1)(1 + sT_3)}{(1 + sT_w)(1 + sT_2)(1 + sT_4)},$$

such that a voltage signal $\Delta V_s(s) = G_{stab}(s)\Delta\omega(s)$ is delivered to the exciter. The exciter also receives the change in magnitude of the terminal voltage $\Delta|V_a|$. Here we use an IEEE AC4A exciter, which has the transfer function

$$G_x(s) = \frac{K_A(1 + sT_C)}{(1 + sT_A)(1 + sT_B)}$$

that characterizes the relation between the change in field-winding voltage ΔE_{fd} and the change in exciter input voltage ΔV_I. Moreover, the generator has a flux decay transfer function

$$G_{flux}(s) = \frac{K_3}{1 + K_3\tau_{d0}'s}$$

such that the change in stator voltage magnitude $\Delta|E_a'|(s) = G_{flux}(s)\Delta E_{fd}'(s)$, where $\Delta E_{fd}' = \Delta E_{fd} - K_4\Delta\delta$, i.e., the

TABLE I
PARAMETERS USED IN THE CASE STUDIES

Param.	Value	Param.	Value (s)	Param.	Value (s)
K_A	200	H	5	T_1	0.2
K_1	1.0755	T_A	0.04	T_2	0.02
K_2	1.2578	T_B	12	T_3	0.4
K_3	0.3072	T_C	1	T_4	0.04
K_4	1.7124	τ'_{d0}	5.9	T_w	10
Param.	Value	Param.	Value (s)	Param.	Value (pu)
K_5	-0.0409	T_G	0.2	D	1
K_6	0.4971	T_{CH}	0.3	R	0.05
K_w	20	T_{RH}	7	F_{HP}	0.3

rotor angle $\Delta\delta$ has a negative feedback to the field-winding voltage. We have the transfer function of M_2, denoted by G_2, as

$$G_2(s) = \frac{G_1(s)}{1 - G_1(s)[F(s) + K_1/s]},$$

where $G_1(s)$ is given in (18) and $F(s)$ is (omitting the (s) following the transfer functions and variables for simplicity)

$$F = \frac{K_2\Delta|E'_a|}{\Delta\omega}$$
$$= \frac{K_2 G_{flux}(-K_5 G_x/s - K_4/s + G_x G_{stab})}{1 + K_6 G_{flux} G_x}.$$

The system under consideration is a per unit system with baseline power $P_{base} = 2000$ MVA. The sampling time is $\Delta t = 0.1$ s. There are N loads in each experiment. Load $i \in I = \{1, 2, ..., N\}$ has a disutility function $D_i(\Delta d_i) = (1/2)\overline{\alpha}_i\Delta d_i^2$, where $\overline{\alpha}_i$ is a random number, e.g., uniformly distributed on $[1, 3]$ in our experiments. For $i \in I$, $\Delta d_i \in [0, \overline{d}_i]$, where $\overline{d}_i$ is a positive random number and $\sum_{i \in I} \overline{d}_i = 0.30$ per unit (pu). In the asynchronous setting, the upper bound for all frequency measurement delays is $\overline{r} = 2$ (see Assumption 4 for $\overline{r}$), and the set of decision times of load i is $T_i = T = \{1, 2, 3, ...\}$ for $i \in \{1, ..., N/4\}$, $T_i = \{5, 10, 15, ...\}$ for $i \in \{N/4 + 1, ..., N/2\}$, $T_i = \{10, 20, 30, ...\}$ for $i \in \{N/2 + 1, ..., 3N/4\}$, and $T_i = \{50, 100, 150, ...\}$ for $i \in \{3N/4+1, ..., N\}$. All loads run the load control algorithm with the stepsize $\gamma = 0.9/(\overline{\alpha}N/2+2\overline{r})$, where $\overline{\alpha} = \max_{i \in I} \overline{\alpha}_i$. Therefore, all the sufficient conditions for the convergence of Algorithms 1 and 2 are satisfied. Table I gives the other parameters values used in the case studies.

B. Generation-loss like contingencies

We use the disturbance Δg which contains two step changes to resemble generation-loss like contingencies, and observe the performance of the proposed load control scheme. Δg is initially zero. At time $t = 2$ s, the first step change occurs with Δg falling by 0.05 pu; at $t = 20$ s, the second step change occurs with Δg falling further by 0.20 pu.

Figure 4 shows the frequency response of the complete system model M_2 to the step changing disturbance, with the synchronous or the asynchronous algorithm. Both algorithms improve the frequency response with small deviations from
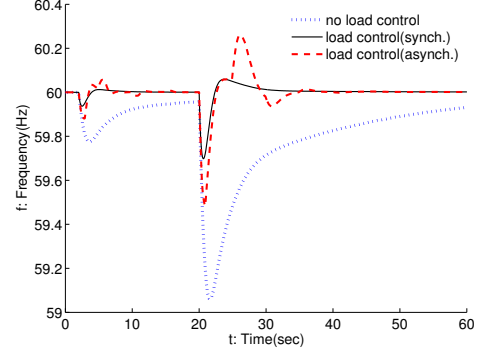

Fig. 4. Frequency reponse with the synchronous or the asynchronous algorithm. The dotted line is the frequency response without load control. The solid line and the dashed line are respectively the frequency response with load control using the synchronous and the asynchronous algorithm.
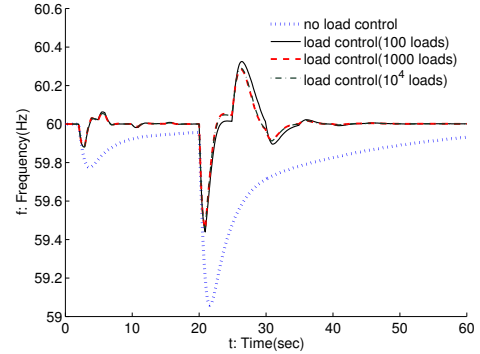

Fig. 5. Frequency reponse with different numbers of loads. The dotted line is the frequency response without load control. The solid line, the dashed line and the dash-dot line are respectively the frequency response with load control algorithms applied on 100, 1,000 and 10,000 loads.

and quick convergence (within 10 s after the first generation fall and 20 s after the second) to 60 Hz. The synchronous algorithm performs better with even smaller oscillations in transient frequency response than the asynchronous algorithm, because in the synchronous algorithm all the loads are adjusted to the optimal power given the newest gradient value simultaneously at every sampling time, while in the asynchronous algorithm loads get delayed gradient value and some loads are not adjusted at some times.

Figure 5 shows the frequency response of the complete system model M_2 to the step changing disturbance, with the asynchronous algorithm applied on different numbers of loads. We see that the number of loads does not affect the frequency response very much. As the number of loads increases, the proposed load control scheme maintains its response speed and convergence rate as there is a small number of loads. In other words, decentralization to more loads does not compromise the performance of the proposed load control scheme.

Now we discuss the effect of using a simplified model instead of an accurate model in the load control scheme. In both Algorithms 1 and 2, a discrete-time realization of
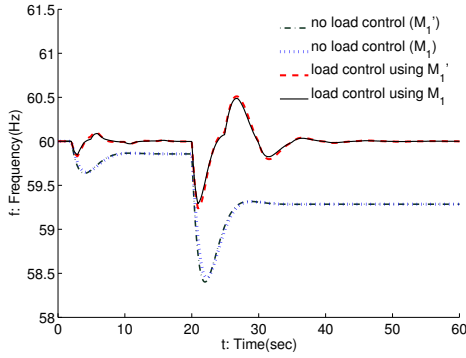
Fig. 6. Frequency reponse of the core part model M_1 and the simplified model M_1'. The dotted line and the dash-dot line are respectively the frequency response of M_1 and M_1' without load control. The solid line and the dashed line are respectively the frequency response of M_1 with load control using M_1 and using M_1'.

the system model, denoted by $\{A, B, C\}$, is given to every load. However, as is mentioned in Section I, users may not get an accurate model, since the utility company may not reveal the exact system information to the public for security considerations, and the accurate model may be so complicated that it costs much to determine it, deliver it to users and compute with it. Hence, we consider the effect of using a simplified model in the load control algorithm.

For the complete system model M_2, we derive its simplifed model from its core part M_1, since M_1 captures the main characteristics of the frequency response. Note that the transfer function of M_1, denoted by G_1, has a pair of conjugate complex poles which are close to the imaginary axis for the given parameter values. With this condition, we simplify G_1 by discarding poles and zeros that are far from the imaginary axis and canceling zero-pole pairs that are close to each other [28], and have a simplified transfer function

$$\widetilde{G}_1(s) = -\frac{0.1555s + 0.0222}{s^2 + 0.9918s + 0.4666}.$$

which describes a simplified model M_1'. Figure 6 compares the frequency response of M_1 and M_1'. As we can see, M_1' approximates M_1 very well, since its frequency response curve without load control almost overlaps with that of M_1, and the frequency response curves with load control using M_1 and M_1' are quite similar. Hence, M_1' can be regarded as a simplification of the core part model M_1, and a simplification of the complete model M_2.

Figures 7-9 respectively compare the frequency response, the total change in load and the disutility with load control schemes using the complete model M_2 and the simplified model M_1'. Comparing the no-load-control frequency response curves of M_2 (the dotted line) and M_1' (the dash-dot line) in Figure 7, we see that M_1' is not an accurate simplification of M_2. However, the frequency response, the total change in load and the disutility with load control schemes using M_2 and M_1' are still quite close (though there are small steady state differences after the second step change
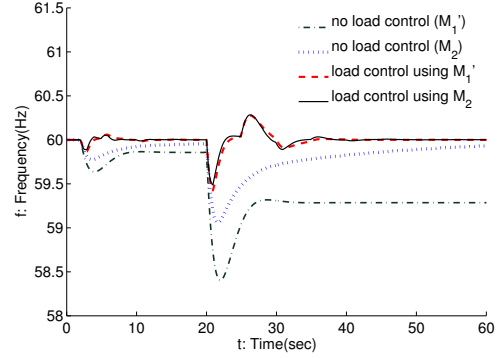

Fig. 7. Frequency reponse with load control schemes using the complete model M_2 and the simplified model M_1'. The dotted line and the dash-dot line are respectively the frequency response of M_2 and M_1' without load control. The solid line and the dashed line are respectively the frequency response with load control schemes using M_2 and using M_1'.
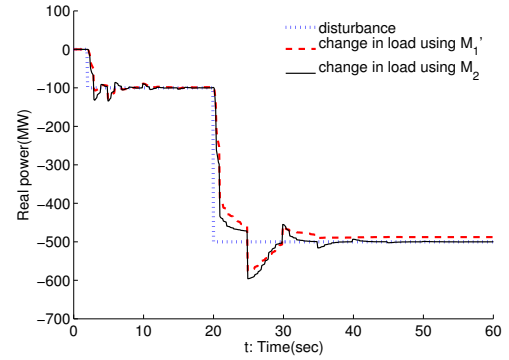

Fig. 8. Total change in load with load control schemes using the complete model M_2 and the simplified model M_1'. The dotted line is the disturbance Δg. The solid line and the dashed line are respectively the total change in load with load control schemes using M_2 and using M_1'.
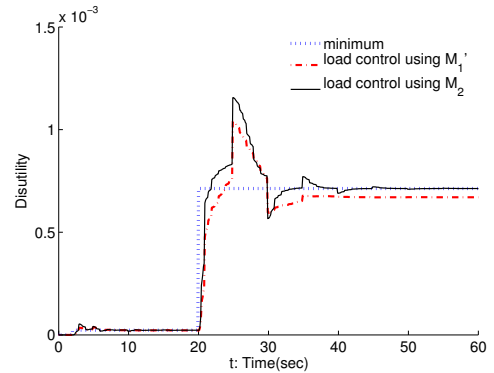

Fig. 9. Disutility caused by load control schemes using the complete model M_2 and the simplified model M_1'. The dotted line is the minimal disutility that can be achieved. The solid line and the dashed line are respectively the disutility caused by load control schemes using M_2 and using M_1'.
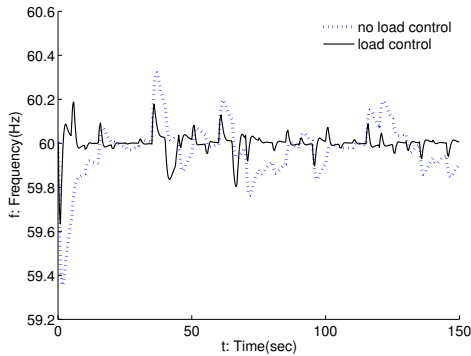
Fig. 10. Frequency reponse to wind power injection. The dotted line and the solid line are respectively the frequency response without load control and with the load control scheme using the asynchronous algorithm.
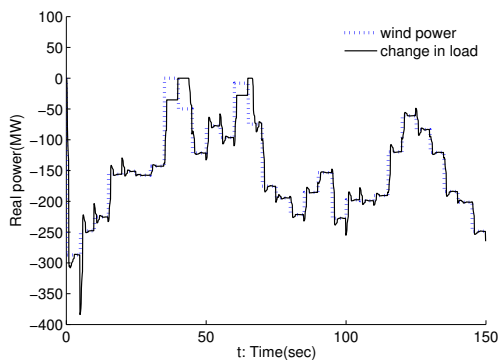

Fig. 11. Total change in load under wind power injection. The dotted line is the wind power generation. The solid line is the total change in load with the load control scheme using the asynchronous algorithm.

in Figures 8 and 9), which implies the proposed scheme is robust to inaccurate model simplifications. Therefore, it is tolerable to use a simplified system model, instead of an accurate one, in the load control scheme.

C. Wind power generation

Now we show the performance of the proposed load control scheme when power generated by a wind turbine is injected to the system. Though we have not theoretically proved any result about the proposed scheme with time-varying disturbance Δg, we test with the wind power generation to see whether the proposed load control scheme does any better than that without load control, as a prelude to studying detailed algorithms serving the control purposes under renewable generations.

The Δg trace, which resembles the wind power generation, comes from actual wind turbine power output data [11]. Δg varies every 5 seconds. Figures 10 and 11 respectively show the frequency response and the total change in load with the load control scheme using the asynchronous algorithm. Figure 10 shows that with the proposed load control scheme the frequency deviation from 60 Hz becomes smaller than that without load control for most of the time. In addition, the largest absolute value of frequency deviation is 0.6463 Hz

without load control and 0.3517 Hz with the proposed load control scheme, nearly 54% of the former. The root of mean square frequency deviation is 0.1348 Hz without load control and 0.0513 Hz with the proposed load control scheme, nearly 38% of the former. Figure 11 shows that with the proposed load control scheme, the total change in load follows the wind power generation quite well. Experiments with other traces of wind power generation show similar results. At least for the cases we test, the proposed load control scheme does better than that without load control in regulating frequency and balancing demand with supply under wind power generation.

V. LIMITATIONS AND EXTENTIONS

The proposed load control scheme has several limitations. First, we characterize the frequency response to demand-supply power imbalance and derive the load control algorithms based on a linearized power system model, which is suitable for small deviations from the operating point but produces large error when the deviations grow large. Second, we do not consider the model error and the process and measurement noise, which may be a significant issue in practice. Third, we only study a simple power system with a single generator and all the loads sensing the same power line frequency, but have not considered the power network composed of multiple interconnected buses at each the frequency may be different.

These limitations motivate some possible extensions based on our work. In the future, we will work on the robustness issue, i.e., study the performance of the frequency-based load control scheme with model error and noise. Moreover, we will study with more detailed and realistic power system model which may be non-linear and contain multiple synchronous machines and buses so that loads at different sites may have different frequency measurements. In that case, some communication may be required to coordinate the actions of different groups of loads. With these considerations the load control scheme design would become more interesting and practical.

VI. CONCLUSION

In this paper, we present a frequency-based load control scheme to balance demand with supply and regulate frequency in power systems. We set up a load control optimization problem with the objective of minimizing the overall end-use disutility and the constraint of demand-supply power balance. We design decentralized algorithms using local frequency measurements to solve the load control optimization problem, and prove the convergence of the algorithms. Numerical experiments show that the proposed load control scheme is able to relatively quickly balance the power demand with supply and restore frequency under generation-loss like contingencies or renewable power generation. In addition, the proposed scheme still has good performance when an inaccurate, simplified system model, instead of an accurate one, is used in the load control algorithm.

APPENDIX A
PROOF OF THEOREM 1

To prove Theorem 1 (convergence of Algorithm 1), we first give two lemmas that show the properties of the dual objective function U. We skip their proofs since the proof of Lemma 1 follows directly from Assumption 2 and the proof of Lemma 2 uses the similar way with the proof of [19, Lemma 2-3].

Lemma 1. Suppose Assumption 2 holds. Then the dual objective function U is concave, continuously differentiable and bounded above over $\mathbb{R}$.

Lemma 2. Suppose Assumptions 2-3 hold. Then for any $p, q \in \mathbb{R}$

$$|U'(q) - U'(p)| \leq \overline{\alpha} N |q - p|,$$

where $\overline{\alpha} := \max_{i \in I} \overline{\alpha}_i$.

Now we complete the proof of Theorem 1. Let $\{p(t), t \in T\}$ denote the sequence generated by the gradient algorithm, and $\{p_i(t), t \in T\}$ denote the sequence generated by load $i \in I$ using Algorithm 1. Recall that by Proposition 1, $p_i(t) = p(t)$ for all $i \in I$ and all $t \in T$. By Lemma 1-2, the dual objective function U is concave and bounded above, and U' is Lipschitz continuous over $\mathbb{R}$. Following [20, pp. 203-204], if $0 < \gamma < 2/(\overline{\alpha} N)$, then

$$\lim_{t \to \infty} U'(p_i(t)) = 0.$$

Let p^* denote any limit point of $\{p_i(t), t \in T\}$, then $U'(p^*) = 0$. Since U is concave over $\mathbb{R}$ and the dual problem **DP** is unconstrained, p^* is a maximizer of **DP**. It is easy to see that the level set $\{p \in \mathbb{R} | U(p) \geq U(p_i(0))\}$ is compact. Moreover, $U(p_i(t))$ is non-decreasing [20, pp. 204]. Thus $p_i(t)$ is always in a compact set for all t. By the definition of compactness, there exists at least one limit point of $\{p_i(t), t \in T\}$, denoted by p^*. By (5), $\Delta d_i(\cdot)$ is continuous over $\mathbb{R}$, thus $\Delta d_i(p^*)$ is a limit point of $\{\Delta d_i(t), t \in T\}$. By strong duality between **PP** and **DP**, $\Delta d(p^*) := [\Delta d_1(p^*), ..., \Delta d_N(p^*)]^T$ is primal optimal since p^* is dual optimal (see Section II-B).

APPENDIX B
PROOF OF THEOREM 2

To prove Theorem 2 (convergence of Algorithm 2), we first show that Algorithm 2 is a special case of the asynchronous flow control algorithm [19, Algorithm A2].

In Algorithm 2, load $i \in I$ generates a sequence

$$U_{i,t} := \hat{u}_0^i(1), ..., \hat{u}_0^i(K_{i,1}), ..., \hat{u}_{t-1}^i(1), ..., \hat{u}_{t-1}^i(K_{i,t})$$

and a sequence

$$P_{i,t} := p_0^i(1), ..., p_0^i(K_{i,1}), ..., p_{t-1}^i(1), ..., p_{t-1}^i(K_{i,t}).$$

We formulate another sequence $\{p(t), t \in T\}$, which starts from $p(0) = 0$ and evloves as

$$p(t) = p(t-1) + \gamma u_{t-1}. \tag{19}$$

Define $\tau(i, t) := \max\{\tau \in T | \tau + r(i, \tau) = t\}$ where $r(i, \tau)$ is load i's measurement delay of $\Delta \omega_\tau$. The following lemma is straightforward from (17), (19) and Proposition 1.

Lemma 3. The sequence $U_{i,t}$ is the same as $u_0, ..., u_{\tau(i,t)-1}$, and the sequence $P_{i,t}$ is the same as $p(1), ..., p(\tau(i,t))$.

Recall that in Algorithm 2, $p_i(t) = p_{t-1}^i(K_{i,t})$. Now we can regarding $p(t)$, u_t, $p_i(t)$ and $\Delta d_i(t)$ respectively as the link price $p_l(t)$, the estimate of gradient $\lambda_l(t)$, the estimate of link price $\hat{p}^s(t)$ and the transmission rate $x_s(t)$ in the asynchronous flow control algorithm [19, Algorithm A2]. We can see that Algorithm 2 is a special case of the asynchronous flow control algorithm. By the proof of [19, Theorem 2], if Assumption 1-5 hold and the stepsize γ satisfies $0 < \gamma < 1/((\overline{\alpha} N/2) + 2\overline{r})$, any limit point (at least one exists) of the sequence $\{(\Delta d(t), p(t)), t \in T\}$ is primal-dual optimal for the problems **PP** and **DP**. If follows that for $i \in I$, any limit point (at least one exists) of the sequence $\{(\Delta d(t), p_i(t)), t \in T\}$ is primal-dual optimal for the problems **PP** and **DP**.

REFERENCES

[1] P. M. Anderson and M. Mirheydar, "An adaptive method for setting underfrequency load shedding relays," *IEEE Trans. on Power Systems*, vol. 7, no. 2, pp. 647-655, 1992.

[2] A. Molina-Garcia, F. Bouffard and D. S. Kirschen, "Decentralized demand-side contribution to primary frequency control," *IEEE Trans. on Power Systems*, vol. 26, no. 1, pp. 411-419, 2001.

[3] D. S. Callaway and I. A. Hiskens, "Achieving controllability of electric loads," *Proceedings of the IEEE*, vol. 99, no. 1, pp. 184-199, 2011.

[4] M. Ilic and Q. Liu, "Toward sensing, communications and control architectures for frequency regulation in systems with highly variable resources," *Control and Optimization Theory for Electric Smart Grids*, New York: Springer, 2011.

[5] D. Trudnowski, M. Donnelly and E. Lightner, "Power-system frequency and stability control using decentralized intelligent loads," in *Proc. of the 2005 IEEE T&D Conf. Expo.*, Dallas, TX, May 2006.

[6] D. Trudnowski, M. Donnelly and E. Lightner, "Power-system frequency and stability control using decentralized intelligent loads: Benefits and pitfalls," in *Proc. of the 2010 IEEE Power and Energy Society General Meeting*, Minneapolis, MN, Jul. 2010.

[7] J. Dong, J. Zuo, L. Wang, K. S. Kook, I. Chung, Y. Liu, *et al.*, "Analysis of power system disturbance based on wide-area frequency measurements," in *Proc. of the 2007 IEEE Power and Energy Society General Meeting*, Tampa, FL, Jun. 2007.

[8] P. Kundur, *Power System Stability and Control*, New York: McGraw Hill, Inc., 1994.

[9] G. Rogers, *Power System Oscillations*. Boston, MA: Kluwer Academic Publishers, 2000.

[10] G. Strbac and ILEX Energy Consulting, *Quantifying the System Costs of Additional Renewables in 2020*. Department of Trade and Industry, London, U.K., 2002.

[11] Z. Xu, J. Ostergaard, M. Togeby, "Demand as frequency controlled reserve," *IEEE Trans. on Power Systems*, vol. 26, no. 3, pp. 1062-1071, 2011.

[12] V. N. Chuvychin, N. S. Gurov, S. S. Venkata and R. E. Brown, "An adaptive approach to load shedding and spinning reserve control during underfrequency conditions," *IEEE Trans. on Power Systems*, vol. 11, no. 4, pp. 1805-1810, 1996.

[13] A. Brooks, E. Liu, D. Reicher, C. Spirakis and B. Weihl, "Demand dispatch: Using real-time control of demand to help balance generation and load," *IEEE Power&Energy Magazine*, vol. 8, no. 3, pp. 21-30, 2010.

[14] F. C. Schweppe, "Frequency Adaptive Power-Energy Re-Scheduler," United States Patent 4317049, 1979.

[15] F. C. Schweppe, R. D. Tabors, J. L. Kirtley, H. R. Outhred, F. H. Pickel and A. J. Cox, "Homeostatic utility control," *IEEE Trans. Power App. Syst.*, vol. PAS-99, pp. 1151-1163, May/Jun. 1980.

[16] P. Taylor, "Increased renewable energy penetration on island power systems through distributed fuzzy load control," in *Proc. Int. Conf. Renewable Energies for Islands: Toward 100% RES Supply*, Chania, Greece, Jun. 2001.

[17] K. Pandiaraj, P. Taylor, N. Jenkins and C. Robb, "Distributed load control of autonomous renewable energy systems," *IEEE Trans. Energy Conv.*, vol. 16, no. 1, pp. 14-19, Mar. 2001.

[18] PNNL, *Grid Friendly^{TM} Controller Helps Balance Energy Supply and Demand*. [Online]. Available: http://www.gridwise.pnl.gov/docs/pnnlsa36565.pdf.

[19] S. H. Low and D. E. Lapsley, "Optimization flow control, I: Basic algorithm and convergence," *IEEE/ACM Trans. on Networking*, vol. 7, no. 6, pp. 861-874, Dec. 1999.

[20] D. Bertsekas and J. Tsitsiklis, *Parallel and Distributed Computation*. Upper Saddle River, NJ: Prentice Hall, 1989.

[21] D. Bertsekas, *Nonlinear Programming*. Nashua, NH: Athena Scientific, 1995.

[22] A. R. Bergen and V. Vittal, *Power Systems Analysis*, 2nd ed. Upper Saddle River, NJ: Prentice Hall, 2000.

[23] P. M. Anderson and A. A. Fouad, *Power System Control and Stability*, Volume 1. Ames, Iowa: The Iowa State University Press, 1977.

[24] S. Gillijns and B. D. Moor, "Unbiased minimum-variance input and state estimation for linear discrete-time systems," *Automatica*, vol. 43, no. 1, pp. 111-116, 2007.

[25] M. Hou and R. J. Patton, "Input observability and input reconstruction," *Automatica*, vol. 34, no. 6, pp. 789-794, 1998.

[26] S. Boyd and L. Vandenberghe, *Convex Optimization*, U.K.: Cambridge University Press, 2004.

[27] L. Gan, U. Topcu and S. H. Low, "Optimal decentralized protocols for electric vehicle charging," to appear in *Proc. 2011 IEEE Conf. Decision and Control*, Orlando, FL, Dec. 2011.

[28] K. J. Astrom and R. M. Murray, *Feedback Systems: An Introduction for Scientists and Engineers*, Princeton, NJ: Princeton University Press, 2008.

[29] W. Rudin, *Principles of Mathematical Analysis*, 3rd ed. New York: McGraw Hill, Inc., 1976.

[30] N. Li, L. Chen and S. H. Low, "Optimal demand response based on utility maximization in power networks," in *Proc. of the 2011 IEEE Power and Energy Society General Meeting*, Detroit, MI, Jul. 2011.

[31] P. Samadi, A. Mohsenian-Rad, R. Schober, V. W. S. Wong, and J. Jatskevich, "Optimal real-time pricing algorithm based on utility maximization for smart grid," in *Proc. 2010 IEEE SmartGridComm*, Gaithersburg, MD, Oct. 2010.